Best Practices for Wake Model and Optimization Algorithm Selection in Wind Farm Layout Optimization

Nicholas F. Baker*, Andrew P. J. Stanley†, Jared J. Thomas‡, and Andrew Ning§
Brigham Young University, Provo, Utah 84602.

Katherine Dykes¶
National Renewable Energy Laboratory, Golden, Colorado 80401

This paper presents the results of two case studies regarding the wind farm layout optimization problem. We asked a general audience to take part in the studies that we designed, and nine individuals participated. Case study 1 considers variations in optimization strategies for a given simple Gaussian wake model. Participants were given a wake model that outputs annual energy production (AEP) with given wind turbine locations. Participants used an optimization method of their choosing to find an optimal wind farm layout. Case study 2 looks at trade-offs in performance resulting from variation in both physics model and optimization strategy. For case study 2, participants calculate AEP using a wake model of their choice while also implementing their chosen optimization method. Participant submissions for optimized turbine locations were then cross-compared by recalculating the AEP using every other participant's wake model. Results for case study 1 show that the best optimal wind farm layouts in this study were achieved by participants who used gradient-based optimization methods. A clear front-runner emerged with the Sparse Nonlinear OPTimizer plus Wake Expansion Continuation (SNOPT+WEC) optimization method, which consistently discovered a higher AEP for each scenario. Results for case study 2 show that for small wind farms with few turbines, turbine placement on the wind farm boundary is superior. Conclusions for case study 2 were drawn from participant cross-comparison of results.

I. Introduction

Optimizing turbine placement within a wind farm is a complex problem characterized by many local minima. The large number of inter-dependent variables involved in wind farm layout optimization (WFLO) create a design space that is difficult to solve reliably. In this study, we designed and conducted a set of case studies to discover superior practices in solving the WFLO problem.

Two approaches have been taken to simplify the WFLO problem, as described by Padrón et al. [1]. The first approach aims at improving the quality of individual models for wind farm attributes, i.e., aerodynamics, atmospheric physics, turbine structures, etc. The second approach is to improve formulating the optimization problem, as well as the algorithms used to solve the optimization [1].

Complex computational methods such as direct numerical simulations (DNS) or large eddy simulations (LES) can be applied to wind turbines in order to better model the aerodynamics of the waked airflow region. But since these methods use the Navier-Stokes equations, the computational time they require for full simulation can be prohibitive. Simplified engineering wake models (EWMs) respond to this weakness by making certain limiting physics assumptions, which result in greatly reduced computational costs [2]. Yet these simpler, less accurate, approximations may lead to inefficient recommendations for turbine placement, due to what can be inaccurate assumptions in specific wind farm scenarios.

Given a single EWM, optimization methods to select ideal turbine locations may be limited by characteristics of the functions governing the model. For example, EWMs that define a discontinuous wind speed behind wind turbines cannot be effectively used with gradient-based optimization methods. Conversely, EWMs for which gradients have not been calculated are limited to gradient-free algorithms, or gradient-based algorithms using finite difference derivatives. Furthermore, within these limitations, different optimization strategies have varying capacity to avoid local optima in the pursuit of a global optimum. Factors such as step size or the "temperature" tolerances in simulated annealing optimization methods can permit algorithms to escape local concavities in a design space in order to pursue a superior optimum.

To better understand the effects of EWMs and optimization algorithms, we have created two case studies. We solicited participant involvement from many different research labs and private companies in industry currently working on both general optimization methods, as well as methods specific to solving the WFLO problem. The first case study isolates optimization techniques for a single simplified EWM; the second case study observes the differences when combining variations in the EWM and optimization method.

Though papers have been published that survey the state of the wind farm optimization (perhaps one of the most notable written by Herbert-Acero reviewing the current methodologies in the field [2]), our case studies are the first time an international collaboration has been conducted to comparatively analyze optimization methods and EWM selection on a representative WFLO problem.

Our case studies are created in support of the International Energy Agency's (IEA's) Wind Task 37 (IEA37). IEA37 coordinates international research activities centered around the analysis of wind power plants as "holistic" systems [3]. Though our case studies concentrate mainly on wake modelling optimization at the farm-level scale, our results still contribute to IEA37's integrated approach [3] to wind energy.

*Masters Student, Brigham Young University Department of Mechanical Engineering
†Ph.D. Candidate, Brigham Young University Department of Mechanical Engineering
‡Ph.D. Student, Brigham Young University Department of Mechanical Engineering
§Assistant Professor, Brigham Young University Department of Mechanical Engineering
¶Senior Engineer, National Wind Technology Center

II. Methodology

To enable production of useful data, our case studies require a model wind farm with characteristics that are simultaneously restrictive enough to maintain simplicity, yet general enough to maintain relevance to more complex and realistic problems. The wind farm scenarios we selected to meet this criteria, and other details relevant to this project as a whole, are described below in Subsection A.

Many factors affect recommendations for superior turbine placement of a proposed wind farm. The two major factors we chose to study are 1) EWM characteristics and 2) optimization algorithm [2]. We designed two case studies in an attempt to quantify the effects of each of these choices.

For the first case study, in which the goal was to isolate variability in the optimization method, we pre-coded a representative wake model as a control variable and permitted participants to use any optimization strategy to alter turbine locations that would deliver the best annual energy production (AEP) for the farm. This is called case study 1 and is described below in Subsection B.

Isolating EWM variability proves more complicated. An EWM's compatibility with gradient-based or gradient-free optimization methods dictates which algorithms can be applied. As such, designing a case study that restricts participants to a single optimization algorithm would unnecessarily limit the scope of EWMs studied. For this reason, our second case study permits not only participant selection of EWM but also implemented optimization algorithm. It is called case study 2 and is described below in Subsection C.

A. Common to Both Case Studies

1. Wind Turbine Specifications

We used IEA's 3.35-MW reference turbine in all wind farms. Its attributes are open source, and it is designed as a baseline for onshore wind turbine specifications [4]. The specifics of the turbine necessary for our simplified version of Bastankhah's Gaussian wake model (used in case study 1) are located in Table 1:

Table 1 Attributes for NREL's 3.35-MW onshore reference turbine

Rotor Diameter	130	m
Turbine Rating	3.35	MW
Cut-In Wind Speed	4	m/s
Rated Wind Speed	9.8	m/s
Cut-Out Wind Speed	25	m/s

Its power curve is defined as:

$$P(V) = \begin{cases} 0 & V < V_{cut\text{-}in} \\ P_{rated}\left(\frac{V - V_{cut\text{-}in}}{V_{rated} - V_{cut\text{-}in}}\right)^3 & V_{cut\text{-}in} \le V < V_{rated} \\ P_{rated} & V_{rated} \le V < V_{cut\text{-}out} \\ 0 & V \ge V_{cut\text{-}out} \end{cases}$$

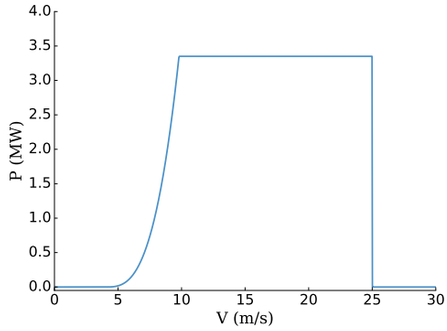

2. Farm Geography

To focus on optimization method and EWM variability, as well as to avoid introducing too many unnecessary variables, the wind farms for all scenarios are on flat and level terrain. To reduce boundary impacts on farm design, we chose a radially symmetric farm boundary. Turbine (x, y) hub locations are restricted to be on or within the boundary radius. Turbines are further constrained to be no less than two rotor diameters apart from any other turbine.

Farm diameter sizing for each scenario needed to be restrictive enough to avoid simply placing all turbines on the boundary yet also permit meaningful turbine movement by the optimizers. Although the participants were not required to use the example starting layouts that we provided, we tried to provide reasonable example layouts by dispersing the turbines as much as possible in an orderly way. This was done by placing turbines in evenly spaced concentric rings. The boundary radii of the various wind farms we defined were selected to permit turbine placement in concentric rings with an average turbine spacing of five rotor diameters.

3. Wind Attributes

The wind distribution frequency and wind speed are the same for all wind farm scenarios in both case studies. Freestream wind velocity is constant in all wind directions, at 9.8 m/s, regardless of turbine location or time of day. This wind speed is used because it is our utilized turbine's rated wind speed. Using this incoming wind velocity increases power production variability experienced by the farm. In setting the scenario's freestream velocity for the turbine's rated wind speed, any wake effects will push air speeds down the turbine's power curve. With greater variability in the resultant produced power, more local optima will be experienced by participant optimizers.

A lack of local optima in a design space permits even ineffective optimizers to find a "best" result. In a design space where local optima are present, inferior designs are very likely. We strove to create such design spaces with our case study scenarios, as they test the robustness of optimization methods.

The selection of wind rose is a major factor in the frequency and magnitude of local optima resulting from turbine placement. We selected a wind rose with an off-axis wind frequency distribution, binned for 16 directions. When we tested this wind rose against 1,000 randomized starting turbine locations, it gave few optimized results with relatively high AEP values. We interpreted this to be indicative of the presence of many local optima. The wind rose we used is depicted in Fig. 1, in polar coordinates. In this figure, a greater magnitude in the radial direction from the origin indicates a higher wind frequency from that specific direction.

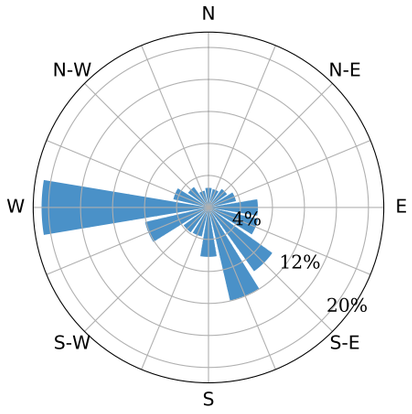

Figure 1 The wind frequency distribution for our case studies

B. Case Study 1: Optimization Only

The purpose of this case study is to determine the best optimization practices for WFLO, using a single representative EWM. We selected a generalized wake model that both gradient-based and gradient-free optimization algorithms could use and that was computationally inexpensive in comparison to LES and DNS methods.

1. Wake Model

The wake model selected for case study 1 is a simplified version of Bastankhah's Gaussian wake model [5, 6]. This wake model is described by the following equations:

$$\frac{\Delta U}{U_\infty} = \left(1 - \sqrt{1 - \frac{C_T}{8\sigma_y^2/D^2}}\right)\exp\left(-0.5\left(\frac{y-\delta}{\sigma_y}\right)^2\right) \tag{1}$$

Where $\frac{\Delta U}{U_\infty}$ is the wake velocity deficit, $C_T = 8/9$ is the thrust coefficient, $y - \delta$ is the distance of the point of interest from the wake center in the cross-stream horizontal direction, D is the turbine diameter, and σ_y is the standard deviation of the wake deficit in the cross-stream horizontal direction as defined in Eq. (2):

$$\sigma_y = (k_y \cdot x) + \frac{D}{\sqrt{8}} \tag{2}$$

In Eq. (2), x is the downstream distance from the turbine generating the wake to the turbine of interest, and D is the turbine diameter. The variable k_y is determined as a function of turbulence intensity (I). In this case study turbulence intensity is treated as a constant of 0.075 (reasonable for an off-shore scenario), and we therefore used a corresponding k_y of 0.0324555 [6, 7].

Increasing turbulence intensity has numerous effects and draws attention away from the main purpose of this case study, which is to observe the differences of optimization strategies. For the wake model we use [given in Eq. (1)], increasing the turbulence intensity widened the wake cone, but second and third order effects are unknown. As such, this first IEA37 set of case studies uses a very low intensity in an attempt to minimize the considered variables.

2. Farm Sizes

Variability in wind farm size (and thus number of design variables) affects optimization algorithm performance. To account for this, three wind farm sizes are specified in case study 1: 16, 36, and 64 turbines. These had farm boundary radii of 1300 m, 2000 m, and 3000 m respectively, determined in the manner described previously in Subsection A.2. Inclusion of three farm sizes is to observe how increased complexity correlates to algorithm performance. The turbine numbers are selected as perfect squares that roughly double in size. Perfect squares are used to permit even grid turbine arrangements, if desired.

3. Supplied Code

To enable participation in this case study, we provided a link to a GitHub repository,* which included files that had:

- Turbine characteristics, wind frequency, and wind speed in IEA 37's `.yaml` schema
- Example turbine layouts for each farm size (in `.yaml` format)
- Python parsers of the `.yaml` schema

*https://github.com/byuflowlab/iea37-wflo-casestudies

- Python target function to calculate AEP (given `.yaml` turbine locations and farm attributes)

We selected the programming language Python, since it is widely used by researchers in the industry.

Participant alteration to our specific code implementation, or replication of our model in another language, was permitted if needed for compatibility with participant optimization methods. This is with the understanding, however, that final wind farm layouts would be evaluated with the original Python code that we provided.

C. Case Study 2: Combined Physics Model/Optimization Algorithm

The intent of this case study is to assess not only the optimization methods measured by case study 1 but also the effects that different physics model approximations have on turbine location recommendations. Case study 2 differs from the previous one in that 1) no wake model is provided and 2) only a single wind farm size is to be optimized. Participants are free to choose their preferred EWM and optimization method combination.

Unlike case study 1, participant-reported AEP is not comparable, since different EWMs are used to calculate them. To help with this, we conducted a cross-comparison of results between participants. For the cross-comparison, each participant's proposed optimal turbine layout in the standardized `.yaml` format was published to the other combined case study participants. Participants then used their own wake model to calculate the AEP of the other participant's proposed farm layouts. From this portion of the case study, we hope to learn if any participants' results are seen as superior by other EWMs.

1. Farm Attributes

The wind farm size for the combined case study is limited to nine turbines. We did this to limit the computation time requirements when assessing results in a standardized LES, discussed later in Section IV. We used the previously described method under Subsection A.2 to determine the boundary radius, and the wind rose and wind speed are the same as case study 1.

III. Results

A. Case Study 1: Optimization Only

Participants ran the optimization algorithm of their choosing using our supplied AEP function or a functional equivalent in another language. Since there exists a great deal of variability in hardware, participants also reported processor speed, function calls, number of cores used, and total Random Access Memory (RAM) installed in their system when finding their optimized results. The AEP results and rankings are given below in Tables 2 to 4.

There were 10 submissions for case study 1. One participant submitted twice, using a different optimization method for each submission. For anonymity, each submission is assigned a number. We will refer to each submission below by this submission number (i.e., *sub1*, ..., *sub10*, etc.).

1. Data

Tables 2 to 4 display the final AEP data of all participant-proposed optimal turbine layouts. The Python module we supplied, which uses the simplified Bastankhah wake model, was used for all AEP calculations. Submissions are ranked from highest to lowest resultant AEP values, with submission number (sub#), whether using a gradient-based (G) or gradient-free (GF) optimization method, and a percentage increase of AEP (Increase) from the provided example layout's AEP.

Table 2 16 turbine scenario participant results

Rank	Algorithm	sub#	Grad.	AEP	Increase
1	SNOPT+WEC	4	G	418924.4064	14.17 %
2	fmincon	5	G	414141.2938	12.86 %
3	SNOPT	8	G	412251.1945	12.35 %
4	SNOPT	1	G	411182.2200	12.06 %
5	Preconditioned Sequential Quadratic Programming	2	G	409689.4417	11.65 %
6	Multistart Interior-Point	10	G	408360.7813	11.29 %
7	Full Pseudo-Gradient Approach	3	GF	402318.7567	9.64 %
8	Basic Genetic Algorithm	7	GF	392587.8580	6.99 %
9	Simple Particle Swarm Optimization	6	GF	388758.3573	5.95 %
10	Simple Pseudo-Gradient Approach	9	GF	388342.7004	5.83 %
11	(Example Layout)	-	-	366941.5712	-

Table 3 36 turbine scenario participant results

Rank	Algorithm	sub#	Grad.	AEP	Increase
1	SNOPT+WEC	4	G	863676.2993	17.05 %
2	Multistart Interior-Point	10	G	851631.9310	15.42 %
3	Preconditioned Sequential Quadratic Programming	2	G	849369.7863	15.11 %
4	SNOPT	8	G	846357.8142	14.70 %
5	SNOPT	1	G	844281.1609	14.42 %
6	Full Pseudo-Gradient Approach	3	GF	828745.5992	12.31 %
7	fmincon	5	G	820394.2402	11.18 %
8	Simple Pseudo-Gradient Approach	9	GF	813544.2105	10.25 %
9	Basic Genetic Algorithm	7	GF	777475.7827	5.37 %
10	Simple Particle Swarm Optimization	6	GF	776000.1425	5.17 %
11	(Example Layout)	-	-	737883.0985	-

Table 4 64 turbine scenario participant results

Rank	Algorithm	sub#	Grad.	AEP	Increase
1	SNOPT+WEC	4	G	1513311.1936	16.86 %
2	Preconditioned Sequential Quadratic Programming	2	G	1506388.4151	16.36 %
3	Multistart Interior-Point	10	G	1480850.9759	14.35 %
4	SNOPT	1	G	1476689.6627	14.03 %
5	Full Pseudo-Gradient Approach	3	GF	1455075.6084	12.36 %
6	SNOPT	8	G	1445967.3772	11.66 %
7	Simple Pseudo-Gradient Approach	9	GF	1422268.7144	9.82 %
8	Simple Particle Swarm Optimization	6	GF	1364943.0077	5.40 %
9	fmincon	5	G	1336164.5498	3.18 %
10	Basic Genetic Algorithm	7	GF	1332883.4328	2.93 %
11	(Example Layout)	-	-	1294974.2977	-

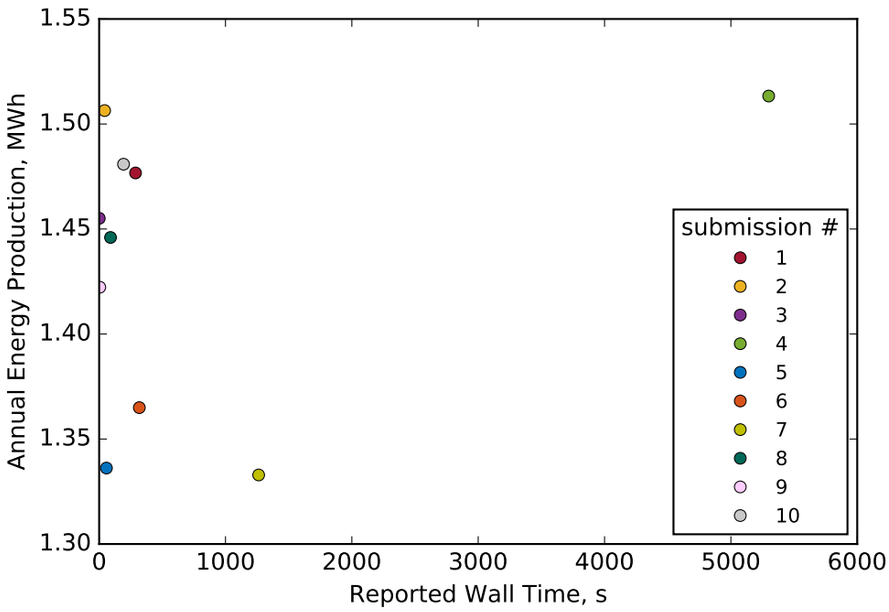

Figure 2 AEP vs reported wall time for each submitted optimization method of the 64 turbine scenario

2. General Trends

As a general trend, gradient-based methods performed better in discovering a relative optima, especially for smaller farm sizes. Some gradient-based algorithms improved in comparative AEP ranking as the number of design variables increases (*sub10*, *sub3*), while others degrade (*sub5*, *sub8*). Simultaneously, one gradient-free algorithm increases in effectiveness as design variables increase (*sub3*), while others compete for lowest comparative performance, regardless of farm size (*sub6*, *sub7*, *sub9*).

Despite these multivariate results, one clear front-runner does emerge. Regardless of wind farm size, *sub4*'s algorithm consistently discovered turbine placements that delivers an AEP superior to all other participants. A summary of *sub4*'s method is included in a following section.

Also of note, as the number of design variables increases, the relative disparity between proposed optimal AEPs likewise diverges. For the 16-turbine case, the highest result is 7.88% better than the lowest. For the 36 and 64 cases, the highest result is 11.45% and 13.54% better than the lowest, respectively.

3. AEP vs Wall Time

Fig. 2 is a plot of AEP from each submission's turbine layout, verses reported wall time for the 64 turbine case, per optimization. Note that in the call for participation, we may not have stressed enough that time and computational expense were important metrics in this study. Therefore, it is possible that many of these reported times were not measured during optimization runs and may have been estimates. Under the premise that these reported times are accurate, Fig. 2 shows the SNOPT+WEC method, though reporting the highest AEP turbine arrangement also may have taken much more time than some other approaches.

More testing could be done to determine if the other methods, when permitted to run longer, would discover an optimum better than that discovered by *sub4*, or if by nature of the algorithms, no matter the time limit permitted to run there are some optima unattainable by their formulations.

4. Analysis of Best Results

For all three farm sizes, the superior method was implemented by *sub4*, using a gradient-based method. Coded in Python and FORTRAN, it combined SNOPT [8] with a method called Wake Expansion Continuation (WEC) [6]. Running 200 optimizations, *sub4* had one optimization run start from the provided example layout, and the other 199 use randomized turbine starting locations within the farm boundary.

The WEC method is specifically designed to reduce the multimodality found in wind farm layout optimization. In the cited paper [6], it is a method of converting design spaces with many local minima into curves approaching convexity, allowing gradient-based optimizations to more easily find the better solutions. An example of such "relaxation" to convexity is included in Figs. 3 and 4, reproduced with permission.

Figs. 3 and 4 demonstrate the effects of the WEC method on a simple design space, relaxing the local optima into a more easily discovered global solution. As the authors Thomas and Ning state, "Larger values of ξ allow the smaller local optima to disappear completely. Smaller values of ξ allow for more accurate wake widths but with an increase in the number and magnitude of local optima." [6]. We suspect that the WEC method for reducing the multimodality of the design space is why *sub4*'s optimizations found superior layouts to the other used methods.

5. Discussion

Though *sub4* consistently found the superior AEP relative to the other participants, *sub2*'s results demonstrate a trend closing the gap as the number of design variables increased. For the 16 turbine case, *sub4* was 2.5% better than *sub2*'s results. For the 36 and 64 cases, *sub4* was 1.68% and 0.46% better, respectively. It should be noted, however, that at the current average U.S. rate [9] of roughly \$0.13 for a kWh (or \$133 per MWh), the income difference between

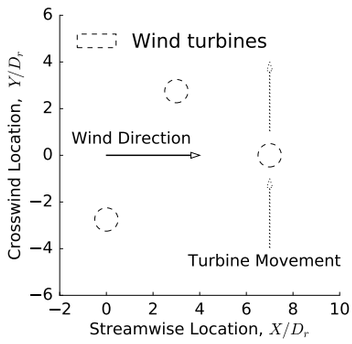

Figure 3 Simple design space used to demonstrate the effects of the relaxation factor, ξ, on the wind farm layout design space. [6]

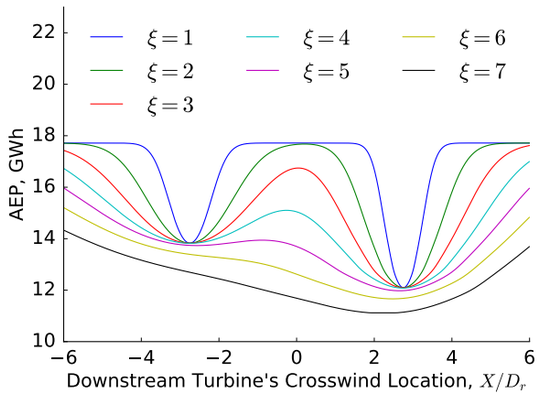

Figure 4 The impact of the wake relaxation factor, ξ. One turbine was moved across the wakes of two upstream turbines (see Fig. 3). [6]

the AEPs of *sub4* and *sub2* in the 64 turbine case, though only 0.46%, equates to a difference of a little under $1 million per year.

Since *sub2*'s Preconditioned Sequential Programming (PSQP) method steadily closed the gap, a future study should test even larger wind farm sizes. This could determine if the PSQP algorithm will eventually outperform the SNOPT+WEC method when a certain number of design variables are reached, or if there is an upper limit or convergence to this trend.

Though the majority of participants used random starts for each optimizaiton, *sub2*'s method of "warm starting" performed progressively well, especially as the number of design variables increased. Taking a starting set of turbine coordinates, *sub2* rotated the layout in $\pi/6$ steps. These rotations created the starting geometry for subsequent iterations. Though not precisely "intuitive" starts, they are more intelligently designed than pure randomized locations. As discussed above, *sub2* did perform increasingly well compared to other methods (ranking 2nd for the 64-turbine case). But more importantly, as can be seen in Fig. 2, *sub2* while getting within 0.46% from the best solution, took less average time per iteration by an order of magnitude. So while the "warm start" rotation method wasn't able to find an AEP superior to *sub4*, it reached an optimized solution much more quickly.

Translating the provided AEP target function proved another sucessful optimization method. At least two participants translated the target Python file into FORTRAN, one into Julia, and one altered it within Python by converting loops into vectorized statements. In testing, this vectorization in Python sped up the computation time by at least an order of magnitude. Similar gains were achieved by the Julia translation, which has built-in vectorization functionality. As demonstrated by these implementations, target function streamlining, either by syntax alteration or programming language translation, proves an effective optimization strategy.

B. Case Study 2: Combined Physics Model/Optimization Algorithm

For case study 2, participants ran both the optimization algorithm and wake model of their choosing. There were no restrictions on programming language for either the wake model or optimization algorithm, but results of optimal turbine layouts were to be submitted in the `.yaml` format supplied in the case study 1 examples.

There were five participant submissions for case study 2. All five participants also submitted for case study 1 (though were not required to do so). For ease of comparison, we assigned their submissions the same numbers from that case study as well (i.e., *sub1* - *sub5* are from the same individual participants for both case study 1 and case study 2).

Because participants used different wake models, AEP values reported cannot be fairly compared between participants. Results were therefore judged on cross-comparison calculations.

1. Data

The cross-comparison displays some interesting trends. Tables 5 to 9 show how each submission's wake models ranked the proposed optimal turbine layouts for the other 4 submissions. Each submission's ranking of its own layout is in **bold**. The penultimate column in each table is the submission number of the layout being cross-compared (cc-sub#). So submission 4's analysis of submission 2's layout would be found in *sub4*'s table, with 2 in the cc-sub# column. The last column is the percentage increase (Increase) from the reporting submission's submitted layout. A negative value here indicates a worse AEP.

Table 5 Cross-comparison results of *sub1*

Rank	Wake Model	Algorithm	AEP	cc-sub#	Increase
1	Simplified Bastankhah	fmincon	262350.319	4	0.624 %
2	Bastankhah	SNOPT+WEC	262282.416	5	0.598 %
3	FLORISSE 3D	SNOPT	**260722.295**	**1**	-
4	Bastankhah	Full Pseudo-Gradient Approach	260640.906	3	-0.031 %
5	Park2	PSQP	248215.024	2	-4.797 %

Table 6 Cross-comparison results of *sub2*

Rank	Wake Model	Algorithm	AEP	cc-sub#	Increase
1	Simplified Bastankhah	fmincon	250464.9732	4	5.975 %
2	Bastankhah	SNOPT+WEC	250249.0259	5	5.884 %
3	Bastankhah	Full Pseudo-Gradient Approach	247812.0522	3	4.853 %
4	FLORISSE 3D	SNOPT	240309.5850	1	1.678 %
5	Park2	PSQP	**236342.799**	**2**	-

Table 7 Cross-comparison results of *sub3*

Rank	Wake Model	Algorithm	AEP	cc-sub#	Increase
1	Bastankhah	SNOPT+WEC	247109.5234	5	0.590 %
2	Simplified Bastankhah	fmincon	246942.3767	4	0.522 %
3	Bastankhah	Full Pseudo-Gradient Approach	**245659.4124**	**3**	-
4	Park2	PSQP	242431.5431	2	-1.314 %
5	FLORISSE 3D	SNOPT	237548.6622	1	-3.302 %

Table 8 Cross-comparison results of *sub4*

Rank	Wake Model	Algorithm	AEP	cc-sub#	Increase
1	Simplified Bastankhah	fmincon	**257790.1924**	**4**	-
2	Bastankhah	SNOPT+WEC	257663.4068	5	-0.049 %
3	Bastankhah	Full Pseudo-Gradient Approach	255063.8201	3	-1.058 %
4	FLORISSE 3D	SNOPT	251776.7157	1	-2.333 %
5	Park2	PSQP	239612.8223	2	-7.051 %

Table 9 Cross-comparison results of *sub5*

Rank	Wake Model	Algorithm	AEP	cc-sub#	Increase
1	Bastankhah	SNOPT+WEC	**251771.9067**	**5**	-
2	Simplified Bastankhah	fmincon	251697.7126	4	-0.029 %
3	Bastankhah	Full Pseudo-Gradient Approach	249829.2199	3	-0.772 %
4	FLORISSE 3D	SNOPT	246503.8323	1	-2.092 %
5	Park2	PSQP	239482.6767	2	-4.881 %

2. General Trends

We expected participants to rank their own layout as superior to the others. Each wake model accounts for different fluids phenomena, and what one wake model considers an optimal layout, another may not. An example of this is if one EWM predicts a wake deficit due to some factor such as vorticity or turbulence. A turbine placed downstream under such a model would, under a more simplistic wake model not accounting for this phenomena (such as the Jensen's model [10]), feel the full brunt of the wake and deliver a suboptimal AEP.

Unexpectedly, only *sub4* and *sub5* found their own layouts to be superior to the other participants. Furthermore, all other participants also found *sub4* and *sub5*'s layouts superior to their own, though to varying degrees. Three participants (including *sub4*) found *sub4* to have the highest AEP-producing layout. The other two participants found *sub5* to have the highest AEP-producing layout.

3. Analysis of Best Results

Within expectations, *sub4* and *sub5* ranked their own layouts superior to all other participant results. Two correlations are important to note regarding *sub4* and *sub5*. First, both used variations of the same wake model. From case study 1, *sub5* used the simplified Gaussian wake model previously described [5, 6]. Though *sub4* also used the Gaussian wake model [5], *sub4* combined it with the model created by Niayifar and Porté-Agel [7], supplemented by the WEC method described earlier. Furthermore, *sub4* also accounted for partial wake, shear, ambient turbulence intensity, and local turbulence intensity. None of these factors were accounted for by *sub5*. The second factor to note is that despite using very similar wake models, *sub4* and *sub5* used different gradient-based optimization algorithms that nonetheless reached very similar conclusions.

As can be seen in the visual depictions included in the Appendix, *sub4* and *sub5* found nearly identical optimal turbine placements. Though appearing identical, the actual coordinates do indeed differ, enough so to result in different AEP calculations shown in the tables above.

Without LES data, the conclusions able to be drawn from the cross-comparison analysis are limited. That both *sub4* and *sub5* were found by the other participant wake models to have superior placement could be a result of either a more efficient optimization method or a better coupling between optimization method and wake model. That these minima existed within the other wake models (resulting in a higher computed AEP by those models), yet were nevertheless undiscovered in their optimizations, is inconclusive in telling us which it is.

Both *sub4* and *sub5* used similar wake models but very different optimization methods. Coding in MATLAB, *sub5* did 1,000 random starts and used MATLAB's fmincon (which uses a finite difference method to find gradients) to optimize for a minimum. Using a combination of Python and FORTRAN, *sub4* ran 1 ordered with 199 random starts for 200 optimizations altogether. SNOPT's SQP algorithm (using algorithmic differentiation to obtain gradients) was *sub4*'s implemented optimizer.

Of note, from trends seen above in case study 1, *sub5*'s optimization methods demonstrate superior performance for small design variable sizes but comparatively degrades as the wind farm size increases. The superior performance of this wake model and optimization method combination for this small farm may not be representative of performance on larger wind farms.

4. Discussion

Participants of earlier case studies were critical of wind farm scenarios where non-novel, simplistic layouts (such as all turbines on the boundary border) are optimal. The small farm radius with few turbines given for this case study seems to have fallen into this category. What is interesting, however, is that three of the five participants were trapped in local optima, and proved blind to optima others found using different physics approximations and optimization methods. Many factors could have led to these shortfalls (i.e., inferior optimization methods, lack of sufficient iterations, lack of sufficient wall time, etc.), and further testing would need to be done to discover which factors majorly contributed to the outcome.

IV. Conclusion

Results from case study 1 show that *sub4*s use of SNOPT+WEC delivers superior results for the tested wind farms with 16, 36, and 64 turbines. Although information on this method is continuing to be produced, the initial paper written by Thomas and Ning[6] describes this method. Time differences displayed in Fig. 2 show that *sub4*'s took one of the comparatively longer amounts of time. However, this required computational time difference must be counterbalanced with resultant AEP improvement. Profitability of which wind farm scenario this method is applied to must be considered to determine if the computational trade-off is worth the extra time it will require. Regarding *sub2*'s PSQP method, though it shows a trend of increased performance that may surpass SNOPT+WEC for wind farms of sizes larger than 64, further testing is required to validate this pattern.

Case study 2 demonstrates that, for wind farms of small area with few turbines, placement on the wind farm boundary delivers superior AEP. Shortcomings in participant pairings of optimization methods were trapped in local optima, however. The lesson learned here is to either train researcher intuition to use such layouts as warm starts or improve optimization methods so that automated optimizers can discover this themselves.

Though we are happy with the level of participation in the case studies, a larger participant sample size with different methods may provide more informative data or display other novel and superior methods. To refine our data collection process, we plan on running another round of results for these case studies in the near future.

Due to the difficulty in comparing the results of different EWMs, we will run all participant-reported optimized turbine locations through an LES. With the inherent bias each EWM has for its own optimized locations removed, reported turbine locations will be measured using the same high-fidelity simulation tool for a comparative AEP. Case study 2 was constructed mainly for this LES wake model evaluation in order to gauge which simplified model is most accurate when compared with a higher-cost computational model. Due to time and computing resource constraints, the authors were unable to run the submitted participant layouts through an LES.

Acknowledgments

This work was authored [in part] by the National Renewable Energy Laboratory, operated by Alliance for Sustainable Energy, LLC, for the U.S. Department of Energy (DOE) under Contract No. DE-AC36-08GO28308. Funding provided by the U.S. Department of Energy Office of Energy Efficiency and Renewable Energy Wind Energy Technologies Office. The views expressed in the article do not necessarily represent the views of the DOE or the U.S. Government. The U.S. Government retains and the publisher, by accepting the article for publication, acknowledges that the U.S. Government retains a nonexclusive, paid-up, irrevocable, worldwide license to publish or reproduce the published form of this work, or allow others to do so, for U.S. Government purposes.

The authors gratefully acknowledge the following individuals, in alphabetical order, as submitting participants in the case study:

- Tim Camp, Director, Turbine Engineering
- Abhinav Prakash, Ph.D. Student, Texas A&M University
- Erik Quaeghebeur, Dr.ir, Delft University of Technology
- Sebastian, Sanchez Perez Moreno, Ph.D. Student, Delft University of Technology
- Landon Wiley, M.Sc Student, Brigham Young University

Pictorial Representations of Case Study 1's Participant Submissions

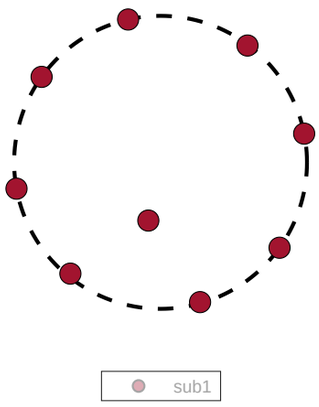

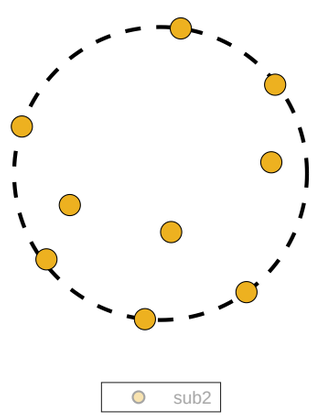

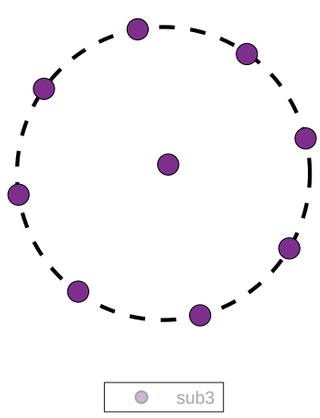

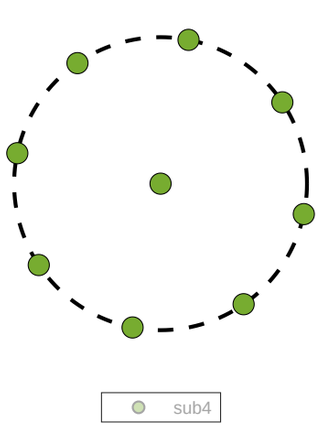

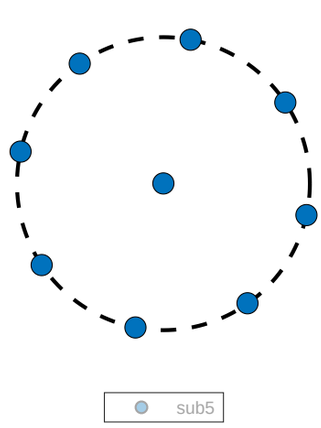

Pictorial Representations of Case Study 2's 16-Turbine Submissions

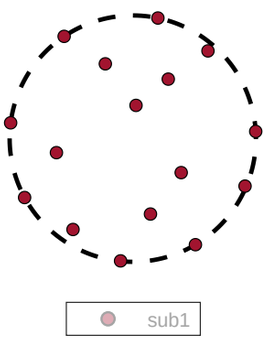

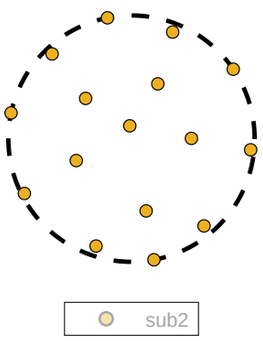

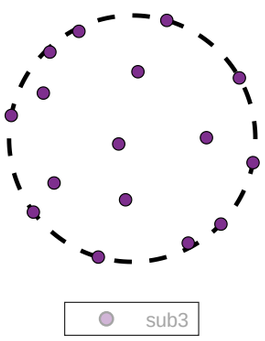

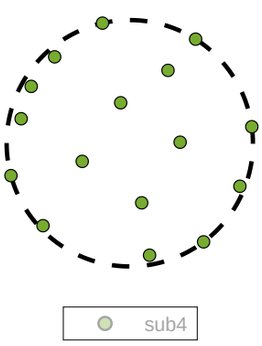

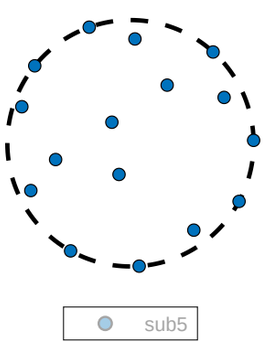

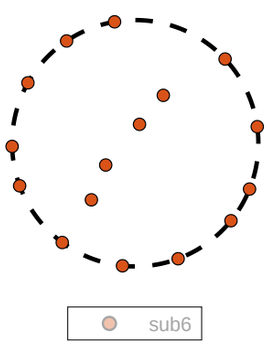

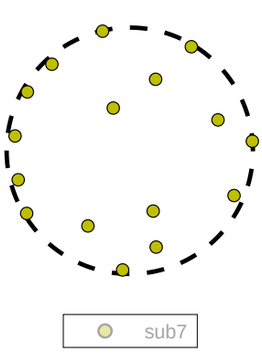

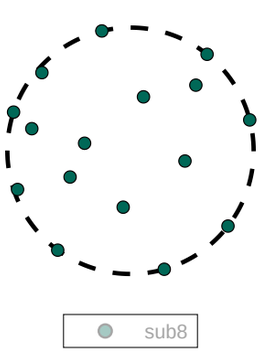

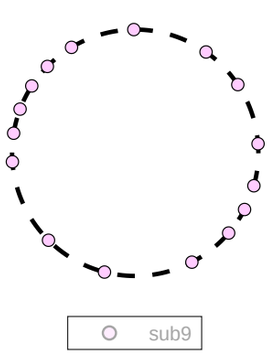

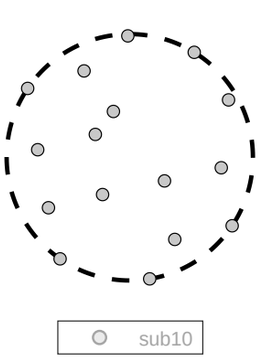

Pictorial Representations of Case Study 2's 36-Turbine Submissions

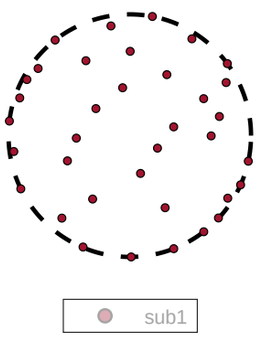

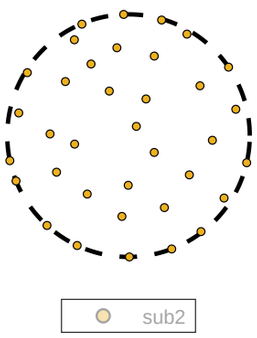

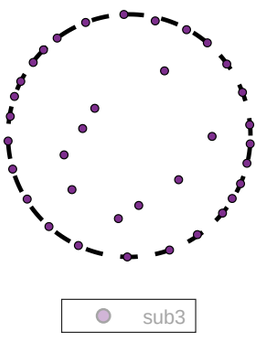

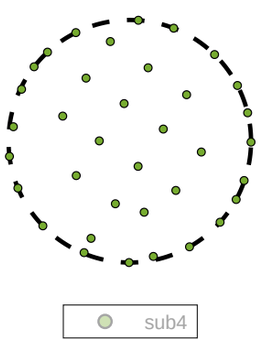

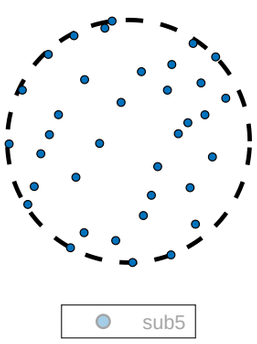

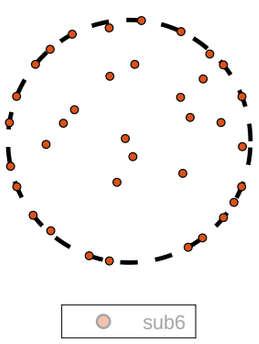

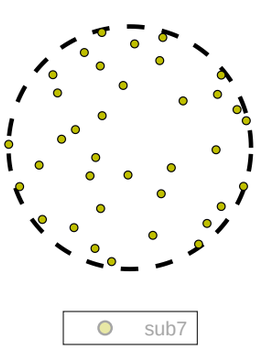

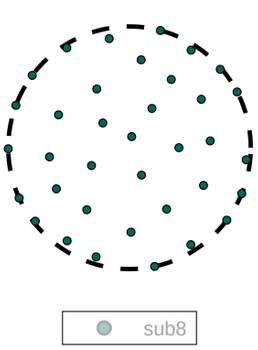

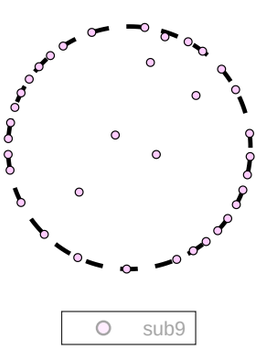

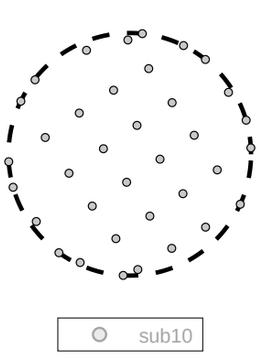

Pictorial Representations of Case Study 2's 64-Turbine Submissions

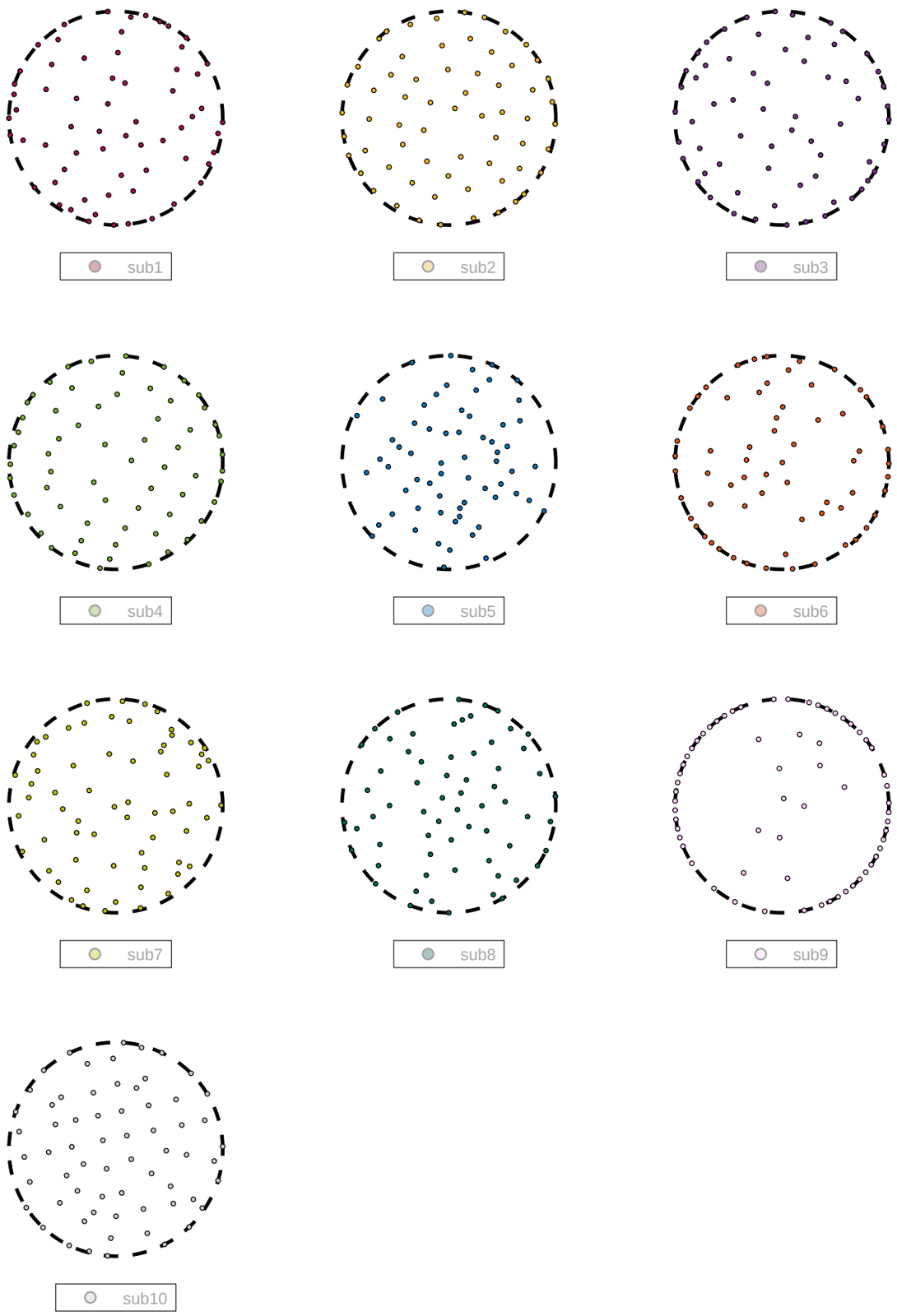

References

[1] Padrón, A. S., Thomas, J., Stanley, A. P. J., Alonso, J. J., and Ning, A., "Polynomial Chaos to Efficiently Compute the Annual Energy Production in Wind Farm Layout Optimization," *Wind Energy Science*, 2018. doi:10.5194/wes-2017-56, (in review).

[2] Herbert-Acero, J. F., Probst, O., Réthoré, P.-E., Larsen, G. C., and Castillo-Villar, K. K., "A Review of Methodological Approaches for the Design and Optimization of Wind Farms," *Energies*, 2014, p. 23.

[3] McWilliam, M. K., Zahle, F., and Dykes, K., "IEA Task 37 on System Engineering in Wind Energy The Aerodynamic Only Optimization Case Study," , May 2017.

[4] Bortolotti, P., Dykes, K., Merz, K., Sethuraman, L., and Zahle, F., "IEA Wind Task 37 on System Engineering in Wind Energy, WP2 - Reference Wind Turbines," Tech. rep., National Renewable Energy Laboratory (NREL), Golden, CO., May 2018.

[5] Bastankhah, M., and Porté-Agel, F., "Experimental and theoretical study of wind turbine wakes in yawed conditions," *J. Fluid Mech.*, Vol. 806, 2016, pp. 506–541.

[6] Thomas, J. J., and Ning, A., "A Method for Reducing Multi-Modality in the Wind Farm Layout Optimization Problem," *Journal of Physics: Conference Series*, Vol. 1037, The Science of Making Torque from Wind, Milano, Italy, 2018, p. 10.

[7] Niayifar, A., and Porté-Agel, F., "Analytical Modeling of Wind Farms: A New Approach for Power Prediction," *Energies*, 2016.

[8] Gill, P., Murray, W., and Saudners, M., "SNOPT: an SQP algorithm for large-scale constrained optimization," *SIAM Review*, Vol. 47, 2005, pp. 99–131.

[9] "Worth of kWh per state," , November 2018. URL `https://www.chooseenergy.com/electricity-rates-by-state/`.

[10] Jensen, N., "A Note on Wind Generator Interactions," Tech. rep., RISO National Laboratory, 1983.